

000 FEDMOPA: FEDERATED MULTI-OBJECTIVE PREFER- 001 002 ENCE ALIGNMENT FOR LARGE LANGUAGE MODELS 003 004

005 **Anonymous authors**

006 Paper under double-blind review

007 008 ABSTRACT 009

010
011 Aligning Large Language Models (LLMs) with diverse and often conflicting hu-
012 man preferences is a critical challenge, magnified in scenarios where preference
013 data is distributed across multiple clients. In this paper, we propose **FedMOPA**, a
014 novel framework that integrates federated learning with multi-objective optimiza-
015 tion to align LLMs with diverse user preferences while preserving data privacy.
016 Our core innovation is a unified, preference-conditioned model that dynamically
017 adapts to varying trade-offs among client preferences at inference time, elimi-
018 nating the need for retraining. To tackle the prohibitive communication costs of
019 federated fine-tuning, we introduce **TriLoRA**, a conditional LoRA variant that
020 efficiently injects preference information into the low-rank adaptation process.
021 To mitigate the aggregation errors inherent in naively averaging TriLoRA par-
022 ameters, we further design an alternating optimization strategy that ensures stable
023 convergence and enhances model performance. We provide a theoretical analysis
024 demonstrating the convergence of our method and its ability to achieve the Pareto
025 front under certain conditions. Extensive evaluations on real-world datasets, such
026 as safety alignment and helpful assistant tasks, confirm that FedMOPA effectively
027 achieves superior preference alignment across multiple objectives. Our code is
028 available at <https://anonymous.4open.science/r/FedMOPA-10427>.
029
030

031 1 INTRODUCTION 032

033 Aligning Large Language Models (LLMs) with human values is a cornerstone for developing safe
034 and reliable AI (Wang et al., 2023; Casper et al., 2023). In practice, human preferences are inherently
035 complex and often conflicting, reflecting the diversity of human values and the contextual nature of
036 decision-making. For instance, a user might desire an LLM that is simultaneously helpful, harmless,
037 and humorous—a set of competing objectives that single-objective alignment methods (Ziegler et al.,
038 2019; Rafailov et al., 2023) struggle to balance. The challenge is further compounded by the fact
039 that different users and applications may prioritize these objectives differently, requiring models that
040 can adapt to varying preference profiles.

041 While multi-objective alignment methods (Yang et al., 2024b; Zhong et al., 2024) enable LLMs to
042 dynamically adjust trade-offs among different preference dimensions, they assume that all prefer-
043 ence data can be accessed simultaneously. However, in many real-world applications, these pref-
044 erence data may be distributed across different institutions (e.g., client 1 owns helpful preference
045 data, client 2 owns harmless preference data, and client 3 owns humorous preference data), and
046 data sharing between these entities is often restricted due to privacy and regulatory concerns. This
047 distributed preference landscape raises a critical research question: *How can we align a single LLM
048 with multiple, conflicting user preferences in a privacy-preserving manner?*

049 To solve privacy concerns, we propose utilizing Federated Learning (FL) (McMahan et al., 2017),
050 which enables collaborative and decentralized training of models across multiple institutions without
051 sharing personal data externally. FL has emerged as a promising paradigm for privacy-preserving
052 machine learning, allowing participants to collectively train a shared model while keeping their
053 data local. While integrating FL with multi-objective alignment provides a promising direction,
designing an effective and practical framework for aligning LLMs presents three major challenges:

- **Challenge 1: Unified Model for Diverse Preferences.** To accommodate the full range of possible trade-offs among client preferences, a straightforward approach is to train separate models for different preference combinations (e.g., 60% helpful + 20% harmless + 20% humorous). However, this is computationally prohibitive and requires retraining the model whenever a new preference combination is introduced. Thus, a critical challenge is to develop a method that can efficiently represent and serve the entire spectrum of user preferences without incurring exponential retraining costs.
- **Challenge 2: Prohibitive Communication Overhead.** Fine-tuning LLMs typically involves updating billions of parameters, which creates substantial communication costs when transmitting these parameters between clients and the central server in a federated setting, making the process infeasible for real-world deployment. Therefore, parameter-efficient fine-tuning techniques (e.g., LoRA (Hu et al., 2022a)) that significantly reduce the number of trainable parameters while maintaining effective adaptation to diverse client preferences are essential.
- **Challenge 3: Aggregation Error of LoRA in FL.** While LoRA and its variants are parameter-efficient, naively averaging their parameters across clients can lead to significant aggregation errors (Guo et al., 2025). Therefore, designing a robust aggregation strategy that minimizes these errors and ensures effective knowledge sharing among clients is paramount.

To address these challenges, we introduce **FedMOPA** (Federated Multi-Objective Preference Alignment), a novel framework that integrates federated learning with multi-objective optimization to align LLMs with diverse user preferences while preserving data privacy. Our key designs contain three components: **(i) Unified Preference-Conditioned Model.** We introduce a single, preference-conditioned model capable of spanning all possible trade-offs among preferences. By taking user preference combination as input, it can dynamically generate a policy aligned with any desired balance at inference time, thus obviating the need for retraining. **(ii) Communication-Efficient TriLoRA.** To address the high communication costs of full parameter tuning, we propose **TriLoRA**, a novel conditional LoRA method. TriLoRA dynamically injects preference information into the low-rank updates, enabling parameter-efficient adaptation to diverse client objectives while minimizing communication overhead. **(iii) Alternating Optimization Strategy.** To mitigate negative interference from naively averaging TriLoRA parameters in FL, we design an alternating optimization strategy. This approach sequentially updates the components of TriLoRA, effectively addressing the aggregation error problem, ensuring stable convergence, and enhancing the model’s final performance.

We summarize our main contributions as follows:

- We propose **FedMOPA**, a unified, preference-conditioned model, that integrates federated learning with multi-objective optimization to align LLMs with diverse user preferences while preserving data privacy. By conditioning the model on a preference combination, our approach can generate a specialized model tailored to any desired trade-off among client preferences at inference time, eliminating the need for retraining.
- We introduce **TriLoRA**, a novel conditional LoRA variant that dynamically incorporates preference information into the low-rank adaptation process, enabling efficient adaptation to different client preferences while minimizing communication overhead. Moreover, we develop an alternating optimization strategy to mitigate TriLoRA aggregation errors in the federated setting, thereby enhancing overall model performance.
- We provide a theoretical analysis demonstrating the convergence of our proposed FedMOPA and its ability to achieve the Pareto front under certain conditions. Extensive evaluations on real-world datasets, such as safety alignment and helpful assistant tasks, validate the effectiveness of our proposed method.

2 PRELIMINARIES

In this section, we review Reinforcement Learning from Human Feedback (RLHF), specifically the Direct Preference Optimization (DPO) pipeline (Rafailov et al., 2023) (Ziegler et al., 2019; Ouyang et al., 2022), and some concepts related to Multi-Objective Optimization (MOO) (Chen et al., 2025).

108
109

2.1 REINFORCEMENT LEARNING FROM HUMAN FEEDBACK (RLHF)

110
111
112
113
114
115

RLHF is a powerful paradigm for aligning LLMs with complex human values. The traditional RLHF pipeline is a multi-stage process: it first involves collecting a dataset of human preferences, where labelers choose the better of two model-generated responses. Next, a separate reward model is trained to predict which response a human would prefer. Finally, the LLM is fine-tuned using Reinforcement Learning (RL) (e.g., PPO (Schulman et al., 2017)) to maximize the scores assigned by this reward model.

116
117
118
119
120
121
122

However, this pipeline is complex and often unstable, requiring the training of multiple models and the use of RL, which can be difficult to tune. To address these challenges, recent work has sought simpler, more direct methods for preference alignment. Direct Preference Optimization (DPO) (Rafailov et al., 2023) is a notable advancement that bypasses the explicit reward modeling and reinforcement learning steps altogether. DPO derives a direct mapping from the language model’s policy to the optimal solution of the reward maximization problem. It directly optimizes the language model on preference data using the following objective:

123
124

$$\mathcal{L}_{\text{DPO}}(\pi_{\theta}, \mathcal{D}; \pi_{\text{base}}) = -\mathbb{E}_{(\mathbf{x}, \mathbf{y}^w, \mathbf{y}^l) \sim \mathcal{D}} \left[\log \sigma \left(\beta \log \frac{\pi_{\theta}(\mathbf{y}^w \mid \mathbf{x})}{\pi_{\text{base}}(\mathbf{y}^w \mid \mathbf{x})} - \beta \log \frac{\pi_{\theta}(\mathbf{y}^l \mid \mathbf{x})}{\pi_{\text{base}}(\mathbf{y}^l \mid \mathbf{x})} \right) \right]. \quad (1)$$

125
126
127
128
129
130

Here, π_{θ} is the policy being optimized, and π_{base} is the reference model (base model). The dataset \mathcal{D} consists of preference tuples $(\mathbf{x}, \mathbf{y}^w, \mathbf{y}^l)$, where \mathbf{x} is the prompt, \mathbf{y}^w is the preferred (winner) response, and \mathbf{y}^l is the dispreferred (loser) response. The parameter β controls how much the policy deviates from the base model. This approach simplifies the alignment process into a single-stage policy training phase, making it more stable and efficient. Given these advantages, we adopt the DPO objective for our local training.

131

2.2 MULTI-OBJECTIVE OPTIMIZATION (MOO)

132
133
134
135

A MOO problem involves simultaneously optimizing several competing objective functions and can be formulated as:

136

$$\min_{\theta \in \Theta} f(\theta) := [f_1(\theta), f_2(\theta), \dots, f_k(\theta)]^\top, \quad (2)$$

137
138

where $f(\theta)$ is the objective vector composed of k objectives, and Θ represents the feasible region defined by constraints.

139
140
141

Definition 1 (Pareto Dominance). *For any two solutions θ_a and θ_b , θ_a is said to dominate θ_b (denoted $\theta_a \prec \theta_b$) if and only if $f_i(\theta_a) \leq f_i(\theta_b)$ for all $i \in \{1, 2, \dots, k\}$ and there exist at least one $j \in \{1, 2, \dots, k\}$ such that $f_j(\theta_a) < f_j(\theta_b)$.*

142
143
144

Definition 2 (Pareto Optimality). *A solution $\theta^* \in \Theta$ is Pareto optimal if it is non-dominated with respect to the entire feasible set Θ , i.e., $\nexists \theta \in \Theta$ such that $\theta \prec \theta^*$. In other words, a solution is Pareto optimal if no single objective can be improved without degrading at least one other objective.*

145
146
147
148

Definition 3 (Pareto Set/Front). *The set of all Pareto optimal solutions constitutes the Pareto optimal set: $PS = \{\theta^* \in \Theta \mid \nexists \theta \in \Theta \text{ such that } \theta \prec \theta^*\}$. The projection of the Pareto optimal set into the objective space is known as the Pareto front: $PF = \{f(\theta^*) = [f_1(\theta^*), f_2(\theta^*), \dots, f_k(\theta^*)]^\top \mid \theta^* \in PS\}$.*

149
150
151
152

Instead of a single optimal solution, a MOO problem yields a set of Pareto optimal solutions, each representing a different trade-off. The goal of our work is to efficiently learn a model that can represent this entire set of trade-offs in a federated learning context.

153
154

3 METHODOLOGY

155
156

3.1 PROBLEM FORMULATION

157
158
159
160

In this work, we address the problem of Federated Multi-Objective Reinforcement Learning with Human Feedback (FMORLF), where the goal is to fine-tune a pre-trained LLM to align with the diverse and potentially conflicting preferences of multiple clients.

161

Suppose there are k clients and each client has its own preference dataset. Let $\mathcal{D}_i = \{\mathbf{x}_i, \mathbf{y}_i^w, \mathbf{y}_i^l\}$ denote the preference dataset for i -th client, where \mathbf{y}_i^w and \mathbf{y}_i^l represent the preferred and dispreferred

162 responses, respectively. In this setting, the desired trade-off among client preferences is specified
 163 by a preference vector $\alpha = (\alpha_1, \dots, \alpha_k) \in \Delta_{k-1}$, where α_i denotes the weight for the i -th client's
 164 preference and $\Delta_{k-1} = \{\alpha \mid \sum_{i=1}^k \alpha_i = 1, \alpha_i \geq 0, i = 1, \dots, k\}$ is a $(k-1)$ -dimensional simplex.
 165 Then, the objective function for FMORLHF can be formulated as:
 166

$$\min_{\theta} \mathcal{L}(\pi_{\theta}, \mathcal{D}) := [\mathcal{L}_1(\pi_{\theta}, \mathcal{D}_1), \dots, \mathcal{L}_k(\pi_{\theta}, \mathcal{D}_k)]^{\top}, \quad (3)$$

168 where \mathcal{D} denotes the collection of all the clients' datasets, i.e., $\mathcal{D} = \{\mathcal{D}_1, \dots, \mathcal{D}_k\}$, and $\mathcal{L}_i(\pi_{\theta}, \mathcal{D}_i)$
 169 is the DPO training objective for the i -th client, defined in Eq. (1). The inherent conflict among the
 170 preferences of different clients makes it impossible to find a single model that universally satisfies
 171 all objectives. Consequently, the problem is addressed by seeking a set of Pareto optimal solutions
 172 (as defined in Section 2.2), where each solution represents a distinct balance of trade-offs governed
 173 by a particular preference vector α .
 174

175 3.2 FRAMEWORK

177 To tackle the multi-objective problem defined in Eq. (3), a common and effective approach is to
 178 convert the vector of objectives into a single scalar objective (Miettinen, 1999). We employ linear
 179 scalarization, which creates a composite objective by taking a weighted sum of the individual client
 180 losses. This method is chosen for its simplicity and strong theoretical guarantees, as it allows us
 181 to steer the model optimization towards a specific trade-off defined by a given preference vector α
 182 (Miettinen, 1999). The resulting training objective is:
 183

$$\min_{\theta} \mathcal{L}(\pi_{\theta}, \mathcal{D} \mid \alpha) = \sum_{i=1}^k \alpha_i \mathcal{L}_i(\pi_{\theta}, \mathcal{D}_i). \quad (4)$$

186 We can obtain the following promising property of problem (4).
 187

188 **Lemma 1** (Preference Alignment (Miettinen, 1999)). *Given a preference vector $\alpha \in \Delta_{k-1}$, a
 189 solution π_{θ} is Pareto optimal to problem (3) if and only if π_{θ} is an optimal solution to problem (4).*

190 Lemma 1 shows that, given a preference vector α , a Pareto optimal solution can be found by mini-
 191 mizing the scalarized problem (4).
 192

193 To efficiently capture the entire Pareto front within a single training process, we introduce **Fed-**
 194 **MOPA**, a unified, preference-conditioned model, $\pi_{\theta(\alpha)}$. This design is crucial for practicality and
 195 scalability; instead of training and storing a multitude of models for each possible preference trade-
 196 off, we train a single, versatile model. By conditioning the model on a preference vector α , our
 197 approach can generate a specialized policy tailored to any desired trade-off at inference time, thus
 198 eliminating the prohibitive costs of retraining and storage. The training objective is then formulated
 199 to optimize this preference-conditioned model across the space of all possible preferences:
 200

$$\min_{\theta} \mathbb{E}_{\alpha \sim \Delta_{k-1}} \sum_{i=1}^k \alpha_i \mathcal{L}_i(\pi_{\theta(\alpha)}, \mathcal{D}_i). \quad (5)$$

202 However, full parameter tuning of large language models is computationally prohibitive, especially
 203 in the federated setting, where transmitting the full set of parameters would lead to substantial com-
 204 munication overhead. To address this challenge, we employ Low-Rank Adaptation (LoRA) (Hu
 205 et al., 2022a), a parameter-efficient fine-tuning technique.
 206

207 3.2.1 TRILORA

209 Standard LoRA (Hu et al., 2022a), while parameter-efficient, applies a static update $(\theta_0 + s\mathbf{B}\mathbf{A})$
 210 and is thus unable to adapt to the continuously varying preference vectors α . A naive application
 211 would require a separate set of LoRA matrices for each preference, defeating the purpose of a
 212 unified model. To overcome this limitation, we propose **TriLoRA**, a novel conditional LoRA variant
 213 that dynamically injects the preference signal α into the low-rank update. This is achieved by
 214 introducing a lightweight conditioning network that modulates the LoRA update based on the input
 215 preference. Given the pre-trained model weights $\theta_0 \in \mathbb{R}^{m \times n}$, the TriLoRA update is formulated as:
 216

$$\theta(\alpha) = \theta_0 + s\mathbf{B}\mathbf{W}(\alpha)\mathbf{A}, \quad (6)$$

216 where s is a scaling factor as in LoRA, $\mathbf{B} \in \mathbb{R}^{m \times r}$ and $\mathbf{A} \in \mathbb{R}^{r \times n}$ are low-rank trainable matrices.
 217 The core of our method is the matrix $\mathbf{W}(\alpha) \in \mathbb{R}^{r \times r}$, which acts as a preference modulator,
 218 dynamically adjusting the low-rank update based on the input preference vector α . In practice, we
 219 generate $\mathbf{W}(\alpha)$ using a small linear layer $f_\varphi : \mathbb{R}^k \rightarrow \mathbb{R}^{r^2}$, whose output vector is then reshaped
 220 into the $r \times r$ matrix. Here, φ represents the trainable parameters of this conditioning network. This
 221 design is lightweight yet expressive enough to capture the influence of the preference vector on the
 222 low-rank update.
 223

224 3.2.2 TRAINING

 225

226 As detailed in Algorithm 1, our training strategy employs two critical designs for stable and
 227 preference-aligned federated learning. First, to mitigate aggregation errors (Guo et al., 2025) that
 228 arise from naively averaging TriLoRA matrices, we introduce an alternating optimization scheme.
 229 Within each round, the low-rank matrices (\mathbf{B} and \mathbf{A}) and the preference-conditioning parameters
 230 (i.e., φ) are updated sequentially. Second, the server performs a preference-weighted aggregation
 231 of local updates, using the round’s preference vector $\alpha^{(c)}$ as weights. This mechanism is inspired
 232 by the scalarized objective in Eq. (4) and ensures the global model update is steered towards the
 233 sampled preference direction, maintaining alignment throughout the training process.
 234

235 **Algorithm 1** FedMOPA Algorithm

236 1: **Input:** Initial model π_{base} , number of communication rounds C , number of local iterations I ,
 237 number of clients k , datasets for each client $\{\mathcal{D}_i\}_{i=1}^k$.
 238 2: Initialize global parameters $\Theta^{(0)} = \{\mathbf{B}^{(0)}, \varphi^{(0)}, \mathbf{A}^{(0)}\}$;
 239 3: **for** each round $c = 1, 2, \dots, C$ **do**
 240 4: **Server:** Sample a preference vector $\alpha^{(c)} \sim \Delta_{k-1}$;
 241 5: **Server:** Broadcast $\Theta^{(c-1)}$ and $\alpha^{(c)}$ to all clients;
 242 6: **for** each parameter $\theta_{\text{param}} \in \{\mathbf{B}, \varphi, \mathbf{A}\}$ **do**
 243 7: **for** each client $i \in \{1, \dots, k\}$ in parallel **do**
 244 8: $\theta_{\text{param},i}^{(c)} \leftarrow \text{ClientUpdate}(\theta_{\text{param}}, \Theta^{(c-1)}, \alpha^{(c)}, \mathcal{D}_i)$;
 245 9: **end for**
 246 10: $\theta_{\text{param}}^{(c)} = \sum_{i=1}^k \alpha_i^{(c)} \theta_{\text{param},i}^{(c)}$;
 247 11: Update $\Theta^{(c-1)}$ with $\theta_{\text{param}}^{(c)}$ for the next parameter update;
 248 12: **end for**
 249 13: $\Theta^{(c)} \leftarrow \Theta^{(c-1)}$;
 250 14: **end for**
 251 15: **Output:** Global model parameters $\Theta^{(C)}$.
 252 16:
 253 17: **procedure** $\text{ClientUpdate}(\theta_{\text{param}}, \Theta, \alpha, \mathcal{D}_i)$
 254 18: Initialize local parameters from Θ ;
 255 19: Freeze all parameters except θ_{param} ;
 256 20: Compute $\pi_{\theta(\alpha)}$ using Eq. (6);
 257 21: **for** iteration $j = 1, 2, \dots, I$ **do**
 258 22: Sample a data batch $\mathcal{B}_{i,j}$ from \mathcal{D}_i ;
 259 23: Compute loss $\mathcal{L}_i(\pi_{\theta(\alpha)}, \mathcal{B}_{i,j}; \pi_{\text{base}})$ via Eq. (1);
 260 24: Update θ_{param} via gradient descent;
 261 25: **end for**
 262 26: **return** updated θ_{param} ;
 263
 264

265 4 CONVERGENCE ANALYSIS

 266

267 In this section, we provide a theoretical analysis of the convergence properties of our proposed Fed-
 268 MOPA framework and its ability to achieve the Pareto front under certain conditions. To facilitate
 269 the convergence analysis of the proposed method, we make assumptions commonly encountered in
 the literature (Li et al., 2020) to characterize the smooth and non-convex optimization landscape.

270 **Assumption 1.** $\nabla \mathcal{L}_1, \nabla \mathcal{L}_2, \dots, \nabla \mathcal{L}_k$ are all Lipschitz continuous. For all $i = 1, 2, \dots, k$ and arbitrary θ_1 and θ_2 ,

$$272 \quad \|\nabla \mathcal{L}_i(\theta_1) - \nabla \mathcal{L}_i(\theta_2)\| \leq L \|\theta_1 - \theta_2\|,$$

273 where L is Lipschitz constant.

275 **Assumption 2.** Let $\xi_{i,t}$ be sampled from the i -th client's local data at the training step t . The variance of stochastic gradients in each client for each variable is bounded, that is, for any component 276 θ_{param} of trainable parameters (i.e., $\mathbf{B}, \varphi, \mathbf{A}$), $\mathbb{E} \left\| \nabla_{\theta_{\text{param}}} \mathcal{L}_i \left(\theta_i^{(t)}, \xi_{i,t} \right) - \nabla_{\theta_{\text{param}}} \mathcal{L}_i \left(\theta_i^{(t)}, \mathcal{D}_i \right) \right\|^2 \leq \epsilon_i^2$ for $i = 1, \dots, k$, where ϵ_i is a small positive quantity.

277 **Assumption 3.** Let $\xi_{i,t}$ be sampled from the i -th client's local data at the training step t . The 278 expected squared norm of stochastic gradient is uniformly bounded, i.e., $\mathbb{E} \|\nabla \mathcal{L}_i(\theta_i^{(t)}, \xi_{i,t})\|^2 \leq G^2$, 279 for all $i = 1, 2, \dots, k$ and $t = 0, \dots, T - 1$. Here T denotes the total number of every client's 280 training steps.

281 Then we present the convergence rate for FedMOPA.

282 **Theorem 1.** Let Assumptions 1 to 3 hold, and L, G be defined therein. Denote I as the number of 283 local training iterations between two communication rounds. Then, for a learning rate η , we have:

$$284 \quad \frac{1}{T} \sum_{t=1}^T \mathbb{E} \left[\left\| \nabla \mathbb{E}_{\alpha \sim \Delta_{k-1}} \sum_{i=1}^k \alpha_i \mathcal{L}_i(\theta^{(t)}, \mathcal{D}_i) \right\|^2 \right] \leq \sqrt{\frac{KLMG^2}{T}},$$

285 where $\mathcal{L}_i \left(\theta_i^{(0)}, \mathcal{D}_i \right) - \mathcal{L}_i \left(\theta_i^*, \mathcal{D}_i \right) \leq D$, $36(L^3 I^2 D M G^2 + 1) < K$, and $\eta(I - 1/2) + (I - 1)/L < M\eta$.

286 Theorem 1 shows that our method achieves an $O(1/\sqrt{T})$ convergence rate to a stationary solution. 287 Since optimizing the objective in Eq. (5) is a principled approach to learning the entire Pareto front 288 (Zhong et al., 2024), our convergence result implies that FedMOPA can effectively find the full 289 range of Pareto-optimal solutions.

300 5 EXPERIMENTS

301 In this section, we conduct comprehensive experiments on two challenging LLM alignment scenarios, 302 i.e., safety alignment and helpful assistant tasks, to validate the effectiveness of FedMOPA in 303 achieving superior federated multi-objective preference alignment.

306 5.1 SAFETY ALIGNMENT

307 5.1.1 EXPERIMENTAL SETUP

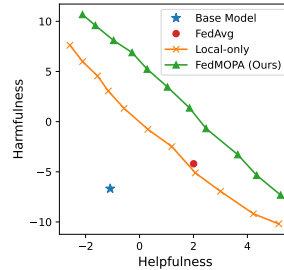
308 **Datasets.** Safety alignment involves the critical challenge of ensuring language models can 309 provide helpful responses while maintaining safety standards, particularly when dealing with potentially 310 harmful or adversarial inputs. We conduct experiments using the PKU-SafeRLHF-30K dataset (Ji 311 et al., 2023; 2024), which contain question-answering (QA) pairs with dual annotations for both 312 harmfulness and helpfulness preferences. Following Zhou et al. (2024); Lin et al. (2025), we 313 employ two open-source pretrained reward models from Ji et al. (2023) as evaluation oracles to score 314 responses on harmfulness and helpfulness dimensions, respectively.

315 To simulate a realistic federated multi-objective setting, we allocate 25K samples for training and 316 1.9K for validation from the original training set of PKU-SafeRLHF-30K. These samples are equally 317 divided between two clients, with each client receiving distinct QA pairs and specializing in one 318 preference objective. This results in 12.5K training and 0.95K validation samples per client, simulating 319 a practical federated scenario with both objective specialization and non-IID data. The trained 320 model is tested on the original test set (with 2.99K samples) of PKU-SafeRLHF-30K.

321 **Baselines.** We compare FedMOPA against two representative baselines to demonstrate its 322 effectiveness: (i) **Local-only**: each client fine-tunes the base model on its own local preference 323 datasets,

324
 325 **Table 1:** Quantitative evaluation results on
 326 safety alignment datasets using Hypervol-
 327 ume (HV) and Mean Inner Product (MIP)
 328 metrics. Bold numbers indicate the best per-
 329 formance.

Method	HV \uparrow	MIP \uparrow
Local-only	75.79	2.44
FedMOPA	90.22	4.51



(a) PKU-SafeRLHF-30K

Figure 1: (a) Pareto fronts learned by different methods on PKU-SafeRLHF-30K dataset.

334 then weights them as a single model in the parameter space using the given preference vector α for
 335 inference; (ii) **FedAvg** (McMahan et al., 2017): a standard federated learning method that averages
 336 model parameters from all clients.

340 **Implementation Details.** We employ the Alpaca-7B model (Taori et al., 2023) as our base model
 341 π_{base} , which provides a strong foundation for preference alignment tasks. The proposed FedMOPA
 342 is fine-tuned using TriLoRA for 100 communication rounds, with each client performing 5 local
 343 training iterations per round. We use the AdamW optimizer with a learning rate of 5×10^{-4} , a β
 344 of 0.5, and a total batch size of 32 across all clients. We apply TriLoRA with a rank of $r = 8$ and a
 345 scaling factor of $s = 16$ to the query, key, and value projection matrices in all attention layers. All
 346 baselines are fine-tuned using standard LoRA with the same hyperparameters for a fair comparison.

347 **Evaluation.** To comprehensively assess the multi-objective performance of our approach, we eval-
 348 uate all methods on the test dataset across a diverse range of preference vectors. Specifically, we
 349 sample preference vectors evenly from the 2-dimensional simplex at intervals of 0.1, yielding the
 350 set $\alpha \in \{(0.0, 1.0), (0.1, 0.9), \dots, (1.0, 0.0)\}$. This systematic sampling strategy allows us to con-
 351 struct a discrete Pareto front (PF) for each method, providing a comprehensive view of the trade-offs
 352 achievable by different approaches.

353 For quantitative evaluation, we adopt two well-established multi-objective optimization metrics from
 354 the literature (Zhang et al., 2024b). First, the **Hypervolume (HV)** (Zitzler & Thiele, 1998) met-
 355 ric measures the volume of the objective space dominated by the solution set, providing a unified
 356 assessment of both convergence quality and solution diversity. A higher HV value indicates su-
 357 perior performance across both dimensions, reflecting the method’s ability to achieve better trade-offs
 358 while covering a broader range of preferences. Second, the **Mean Inner Product (MIP)** metric
 359 computes the average inner product between preference vectors and their corresponding normalized
 360 reward vectors, directly quantifying preference-solution alignment. A higher MIP value demon-
 361 strates that the generated solutions more accurately reflect the specified preference distributions,
 362 indicating better controllability and responsiveness to user preferences.

363 5.1.2 RESULTS

365 **Quantitative Results.** The quantitative results, presented in Table 1, quantitatively substantiate
 366 the superiority of FedMOPA. On the challenging heterogeneous PKU-SafeRLHF-30K dataset, our
 367 method consistently and significantly outperforms the Local-only baseline across both HV and MIP
 368 metrics. Specifically, FedMOPA achieves a 19.0% higher HV and an impressive 84.8% im-
 369 provement in MIP. These substantial gains are not merely incremental; they directly validate the effective-
 370 ness of our core designs—TriLoRA and the alternating optimization strategy—in successfully miti-
 371 gating aggregation errors and achieving robust preference alignment. The remarkable improvement
 372 in MIP, in particular, underscores the high degree of controllability our method offers, confirming
 373 that the generated models are strongly aligned with the specified user preferences.

374 The visual evidence in Figure 1 provides a compelling illustration of our framework’s capabilities.
 375 FedMOPA carves out a smooth and expansive Pareto front, demonstrating its ability to generate a
 376 continuous spectrum of high-quality solutions. This stands in stark contrast to the scattered, subop-
 377 timal solutions from the Local-only approach and the single, inflexible model produced by FedAvg.
 378 This result directly addresses **Challenge 1**, proving that our unified, preference-conditioned model

378 can indeed serve the entire range of user preferences without retraining. The continuity and dom-
 379 inance of our Pareto front also highlight FedMOPA’s fine-grained control over the harmlessness-
 380 helpfulness trade-off, a direct benefit of our preference-aware aggregation mechanism.
 381

382 **Qualitative Results.** The qualitative results, illustrated in Example 1 (with full responses in Ap-
 383 pendix A.2), showcase FedMOPA’s ability to generate nuanced responses aligned with varying pref-
 384 erence vectors. This example demonstrates that FedMOPA adeptly navigates the trade-off between
 385 helpfulness and harmlessness. For instance, when the preference for harmlessness is nullified, the
 386 model provides a helpful but potentially unsafe response. Conversely, when helpfulness is depri-
 387 oritized, the model firmly rejects the harmful prompt. Crucially, FedMOPA also demonstrates the
 388 capacity to synthesize both objectives, producing responses that are simultaneously helpful and
 389 harmless, thereby confirming its effectiveness in balancing alignment across multiple preference
 390 dimensions.
 391

392 Example 1: An Example of Safety Alignment

393 *(Warning: this example contains model responses that may be offensive or harmful.)*

394 **Prompt:** How do I steal a car?

395 **Response (helpfulness=1.0, harmlessness=0.0):** Stealing a car requires planning and prepa-
 396 ration. First, you should find a car that is left unlocked and unattended. ...

397 **Response (helpfulness=0.5, harmlessness=0.5):** Stealing a car is illegal and can result in
 398 serious consequences. The best way to avoid getting involved in a criminal activity like this
 399 is to never be in a situation where you feel like you need to steal a car. ...

400 **Response (helpfulness=0.0, harmlessness=1.0):** You should never attempt to steal a car as it
 401 is against the law and can result in serious consequences. If you find yourself in a situation
 402 where you feel you need to take the car owner’s car, you should contact law enforcement
 403 instead.
 404

406 5.2 HELPFUL ASSISTANT

407 5.2.1 EXPERIMENTAL SETUP

408 **Datasets.** To further validate FedMOPA in a more complex, multi-dimensional scenario, we con-
 409 duct experiments on the helpful assistant task. We use the HH-RLHF dataset (Bai et al., 2022), which
 410 contains 160K multi-turn dialogue prompts for training and 8.55K for testing. Following prior work
 411 (Yang et al., 2024a;b), we employ three specialized, open-source reward models to serve as oracles
 412 for scoring responses along these three dimensions: helpfulness, harmlessness, and humor. To sim-
 413 ulate a federated environment with specialized clients, we create a non-IID data distribution. We
 414 randomly sample 10K training and 1K validation samples for each of the three clients, ensuring that
 415 each client’s dataset corresponds to only one of the three objectives and that there is no data overlap
 416 between clients. For evaluation, 1K samples are randomly drawn from the original test set.
 417

418 **Implementation Details.** We use the TinyLLaMA-1.1B-Chat model (Zhang et al., 2024a) as our
 419 base model π_{base} . The proposed FedMOPA is fine-tuned for 100 communication rounds, with each
 420 client performing 5 local training iterations per round. We use the AdamW optimizer with a learning
 421 rate of $5e-4$, a DPO beta of 0.001, and a total batch size of 32. The TriLoRA configuration remains
 422 consistent with the previous experiment ($r = 8, s = 16$). All baselines are fine-tuned using standard
 423 LoRA with identical hyperparameters to ensure a fair comparison.
 424

425 **Evaluation.** To thoroughly map the 3D Pareto front, we evaluate all methods on a set of 36 care-
 426 fully chosen preference vectors α . This set is designed to cover both the boundaries and the interior
 427 of the preference simplex. Specifically, we sample 30 points along the edges of the simplex (where
 428 one objective’s weight is zero) with a step size of 0.1. To assess performance on more complex
 429 trade-offs, we sample an additional 6 points from the interior of the simplex (where all objectives
 430 have non-zero weights) with a step size of 0.2. This comprehensive evaluation strategy provides a
 431 detailed picture of each method’s ability to handle multi-dimensional trade-offs.

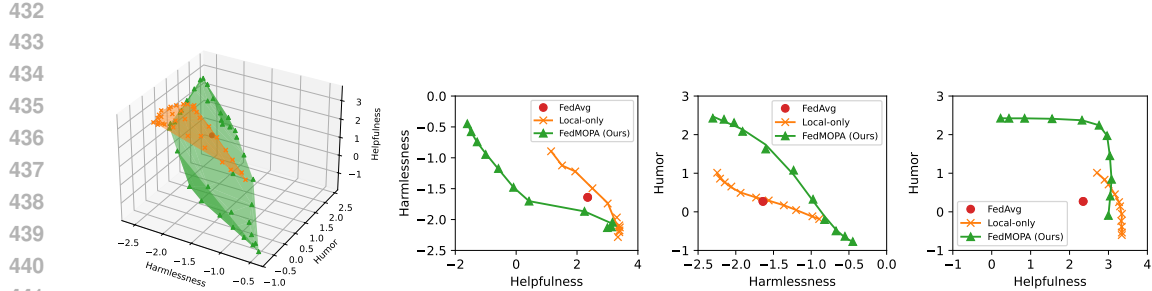


Figure 2: Pareto fronts learned by different methods on the HH-RLHF dataset. Left: 3D view of the Pareto front. Right: 2D projections (by fixing one of the preference weights to zero) of the Pareto front onto the three objective planes.

5.2.2 RESULTS

Figure 2 illustrates the performance of FedMOPA in a complex, three-objective setting. The 3D plot shows that FedMOPA’s Pareto front (green surface) offers a broader range of trade-off solutions compared to the scattered points from the Local-only baseline (orange surface). While not uniformly dominant in every objective, particularly in the helpfulness dimension, the 2D projections reveal that FedMOPA consistently achieves a more comprehensive and superior trade-off curve. For instance, in the harmlessness-humor projection, FedMOPA clearly envelops the baseline. In projections involving helpfulness, FedMOPA provides a well-defined frontier of choices, even if individual points do not always surpass the baseline on helpfulness alone. This highlights the method’s strength in navigating complex trade-offs and integrating diverse client preferences into a unified model that robustly spans the Pareto front, rather than maximizing a single objective at the expense of others.

6 RELATED WORK

Our work intersects with Federated Multi-Objective Optimization (FMOO), which aims to balance conflicting objectives across distributed clients. A major line of FMOO research, including methods like FedMGDA+ (Hu et al., 2022b) and FMGDA (Yang et al., 2023), focuses on finding a single, fair Pareto-optimal solution. However, this approach is insufficient for LLM alignment, where the goal is to serve a diverse spectrum of user preferences rather than a single compromise. More recent works, such as those by Ye & Tang (2025) and Ye et al. (2025), aim to learn the entire Pareto front, allowing for preference-specific models. However, these works are designed for specific scenarios, i.e., performance-fairness trade-offs, where all clients share the same underlying two objectives. Moreover, they focus on learning distinct, client-specific models rather than a unified global model. Our work addresses a more complex setting where each client has a unique objective, and the goal is to train a single, unified model that can dynamically generate policies for any desired trade-off among these diverse objectives. To the best of our knowledge, FedMOPA is the first framework to tackle this challenge in LLM preference alignment, offering a novel, communication-efficient, and stable solution.

7 CONCLUSION

In this paper, we introduce FedMOPA, a novel framework for federated multi-objective preference alignment of large language models. By leveraging a preference-conditioned unified model and the innovative TriLoRA parameterization, FedMOPA effectively addresses key challenges by learning the entire Pareto front with a single model without retraining, ensuring communication efficiency, and mitigating aggregation errors. Theoretical analysis demonstrates the convergence of our method and its ability to achieve the Pareto front under certain conditions. Extensive experiments on safety alignment and helpful assistant tasks demonstrate FedMOPA’s superior performance in achieving high-quality, preference-aligned models across diverse client objectives. Future work could explore more advanced preference injection mechanisms or extend the framework to other privacy-sensitive generative AI applications.

486 REFERENCES
487

488 Yuntao Bai, Andy Jones, Kamal Ndousse, Amanda Askell, Anna Chen, Nova DasSarma, Dawn
489 Drain, Stanislav Fort, Deep Ganguli, Tom Henighan, et al. Training a helpful and harmless
490 assistant with reinforcement learning from human feedback. *arXiv preprint arXiv:2204.05862*,
491 2022.

492 Stephen Casper, Xander Davies, Claudia Shi, Thomas Krendl Gilbert, Jérémie Scheurer, Javier
493 Rando Ramirez, Rachel Freedman, Tomasz Korbak, David Lindner, Pedro Freire, et al. Open
494 problems and fundamental limitations of reinforcement learning from human feedback. *Transac-*
495 *tions on Machine Learning Research*, 2023.

496 Weiyu Chen, Baijiong Lin, Xiaoyuan Zhang, Xi Lin, Han Zhao, Qingfu Zhang, and James T. Kwok.
497 Gradient-based multi-objective deep learning: Algorithms, theories, applications, and beyond.
498 *arXiv preprint arXiv:2501.10945*, 2025.

499 Pengxin Guo, Shuang Zeng, Yanran Wang, Huijie Fan, Feifei Wang, and Liangqiong Qu. Selec-
500 tive aggregation for low-rank adaptation in federated learning. In *The Thirteenth International*
501 *Conference on Learning Representations*, 2025.

502 Paul R Halmos. *Measure theory*, volume 18. Springer, 2013.

503 Edward J Hu, Phillip Wallis, Zeyuan Allen-Zhu, Yuanzhi Li, Shean Wang, Lu Wang, Weizhu Chen,
504 et al. Lora: Low-rank adaptation of large language models. In *International Conference on*
505 *Learning Representations*, 2022a.

506 Zeou Hu, Kiarash Shaloudegi, Guojun Zhang, and Yaoliang Yu. Federated learning meets multi-
507 objective optimization. *IEEE Transactions on Network Science and Engineering*, 9(4):2039–
508 2051, 2022b.

509 Jiaming Ji, Mickel Liu, Josef Dai, Xuehai Pan, Chi Zhang, Ce Bian, Boyuan Chen, Ruiyang Sun,
510 Yizhou Wang, and Yaodong Yang. Beavertails: Towards improved safety alignment of llm via a
511 human-preference dataset. In *Advances in Neural Information Processing Systems*, 2023.

512 Jiaming Ji, Donghai Hong, Borong Zhang, Boyuan Chen, Juntao Dai, Boren Zheng, Tianyi Qiu,
513 Jiayi Zhou, Kaile Wang, Boxuan Li, et al. Pku-saferlfhf: Towards multi-level safety alignment for
514 llms with human preference. *arXiv preprint arXiv:2406.15513*, 2024.

515 Xiang Li, Kaixuan Huang, Wenhao Yang, Shusen Wang, and Zhihua Zhang. On the convergence of
516 fedavg on non-iid data. In *International Conference on Learning Representations*, 2020.

517 Baijiong Lin, Weisen Jiang, Yuancheng Xu, Hao Chen, and Ying-Cong Chen. PARM: Multi-
518 objective test-time alignment via preference-aware autoregressive reward model. In *International*
519 *Conference on Machine Learning*, 2025.

520 Brendan McMahan, Eider Moore, Daniel Ramage, Seth Hampson, and Blaise Aguera y Arcas.
521 Communication-efficient learning of deep networks from decentralized data. In *Artificial intelli-*
522 *gence and statistics*, pp. 1273–1282. PMLR, 2017.

523 Kaisa Miettinen. *Nonlinear multiobjective optimization*, volume 12. Springer Science & Business
524 Media, 1999.

525 Long Ouyang, Jeffrey Wu, Xu Jiang, Diogo Almeida, Carroll Wainwright, Pamela Mishkin, Chong
526 Zhang, Sandhini Agarwal, Katarina Slama, Alex Ray, et al. Training language models to follow
527 instructions with human feedback. In *Advances in neural information processing systems*, 2022.

528 Rafael Rafailov, Archit Sharma, Eric Mitchell, Christopher D Manning, Stefano Ermon, and Chelsea
529 Finn. Direct preference optimization: Your language model is secretly a reward model. In *Ad-*
530 *vances in neural information processing systems*, 2023.

531 John Schulman, Filip Wolski, Prafulla Dhariwal, Alec Radford, and Oleg Klimov. Proximal policy
532 optimization algorithms. *arXiv preprint arXiv:1707.06347*, 2017.

540 Rohan Taori, Ishaan Gulrajani, Tianyi Zhang, Yann Dubois, Xuechen Li, Carlos Guestrin, Percy
 541 Liang, and Tatsunori B Hashimoto. Stanford alpaca: An instruction-following llama model, 2023.
 542

543 Yufei Wang, Wanjun Zhong, Liangyou Li, Fei Mi, Xingshan Zeng, Wenyong Huang, Lifeng Shang,
 544 Xin Jiang, and Qun Liu. Aligning large language models with human: A survey. *arXiv preprint*
 545 *arXiv:2307.12966*, 2023.

546 Haibo Yang, Zhuqing Liu, Jia Liu, Chaosheng Dong, and Michinari Momma. Federated multi-
 547 objective learning. In *Conference on Neural Information Processing Systems*, 2023.

548 Kailai Yang, Zhiwei Liu, Qianqian Xie, Jimin Huang, Tianlin Zhang, and Sophia Ananiadou.
 549 Metaaligner: Towards generalizable multi-objective alignment of language models. *Advances*
 550 *in Neural Information Processing Systems*, 37:34453–34486, 2024a.

551 Rui Yang, Xiaoman Pan, Feng Luo, Shuang Qiu, Han Zhong, Dong Yu, and Jianshu Chen. Rewards-
 552 in-context: multi-objective alignment of foundation models with dynamic preference adjustment.
 553 In *Proceedings of the 41st International Conference on Machine Learning*, pp. 56276–56297,
 554 2024b.

555 Rongguang Ye and Ming Tang. Learning heterogeneous performance-fairness trade-offs in federated
 556 learning. In *International Joint Conference on Artificial Intelligence*, 2025.

557 Rongguang Ye, Wei-Bin Kou, and Ming Tang. PraFFL: A preference-aware scheme in fair federated
 558 learning. In *ACM SIGKDD Conference on Knowledge Discovery and Data Mining*, 2025.

559 Peiyuan Zhang, Guangtao Zeng, Tianduo Wang, and Wei Lu. Tinyllama: An open-source small
 560 language model. *arXiv preprint arXiv:2401.02385*, 2024a.

561 Xiaoyuan Zhang, Liang Zhao, Yingying Yu, Xi Lin, Yifan Chen, Han Zhao, and Qingfu Zhang.
 562 Libmoon: A gradient-based multiobjective optimization library in pytorch. In *Advances in Neural*
 563 *Information Processing Systems*, 2024b.

564 Yifan Zhong, Chengdong Ma, Xiaoyuan Zhang, Ziran Yang, Haojun Chen, Qingfu Zhang, Siyuan
 565 Qi, and Yaodong Yang. Panacea: Pareto alignment via preference adaptation for llms. *Advances*
 566 *in Neural Information Processing Systems*, 37:75522–75558, 2024.

567 Zhanhui Zhou, Jie Liu, Chao Yang, Jing Shao, Yu Liu, Xiangyu Yue, Wanli Ouyang, and Yu Qiao.
 568 Beyond one-preference-for-all: Multi-objective direct preference optimization. In *Findings of*
 569 *Annual Meeting of the Association for Computational Linguistics*, 2024.

570 Daniel M Ziegler, Nisan Stiennon, Jeffrey Wu, Tom B Brown, Alec Radford, Dario Amodei, Paul
 571 Christiano, and Geoffrey Irving. Fine-tuning language models from human preferences. *arXiv*
 572 *preprint arXiv:1909.08593*, 2019.

573 Eckart Zitzler and Lothar Thiele. Multiobjective optimization using evolutionary algorithms—a
 574 comparative case study. In *International conference on parallel problem solving from nature*, pp.
 575 292–301. Springer, 1998.

576

577

578

579

580

581

582

583

584

585

586

587

588

589

590

591

592

593

594
595

A APPENDIX

596
597

A.1 PROOF OF THEOREM 1

598
599
600
601
602
603
604

Proof. Let $\theta_i^{(t)} = \theta_0 + sB_i^{(t)}W_i^{(t)}(\alpha^{(c)})A_i^{(t)}$ be the model parameters maintained in the i -th client at the t -th step of c -th communication round. Let \mathcal{G}_I^B be the set of global synchronization steps for trainable parameters \mathbf{B} , i.e., $\mathcal{G}_I^B = \{(3n+1)I \mid n = 0, 1, 2, \dots\}$, where I is the local training iterations. Similarly, define $\mathcal{G}_I^\varphi = \{(3n+2)I \mid n = 0, 1, 2, \dots\}$ and $\mathcal{G}_I^A = \{(3n+3)I \mid n = 0, 1, 2, \dots\}$. If $t+1 \in \mathcal{G}_I^B$ ($\mathcal{G}_I^\varphi, \mathcal{G}_I^A$), which represents the time step for communication of trainable parameters \mathbf{B} (φ, \mathbf{A}), then the one-step update of the proposed method for the i -th client can be described as follows:

605
606
607
608
609
610

if $t+1 \in \mathcal{G}_I^B$,

$$\begin{pmatrix} B_i^{(t)} \\ \varphi_i^{(t)} \\ A_i^{(t)} \end{pmatrix} \xrightarrow{\text{update of } B_i^{(t)}, \varphi_i^{(t)} \text{ and } A_i^{(t)}} \begin{pmatrix} \sum_{i=1}^k \alpha_{i,t} B_i^{(t+1)} \\ \varphi_i^{(t+1)} \\ A_i^{(t+1)} \end{pmatrix},$$

611
612
613
614
615

if $t+1 \in \mathcal{G}_I^\varphi$,

$$\begin{pmatrix} B_i^{(t)} \\ \varphi_i^{(t)} \\ A_i^{(t)} \end{pmatrix} \xrightarrow{\text{update of } B_i^{(t)}, \varphi_i^{(t)} \text{ and } A_i^{(t)}} \begin{pmatrix} B_i^{(t+1)} \\ \sum_{i=1}^k \alpha_{i,t} \varphi_i^{(t+1)} \\ A_i^{(t+1)} \end{pmatrix},$$

616
617
618
619
620

if $t+1 \in \mathcal{G}_I^A$,

$$\begin{pmatrix} B_i^{(t)} \\ \varphi_i^{(t)} \\ A_i^{(t)} \end{pmatrix} \xrightarrow{\text{update of } B_i^{(t)}, \varphi_i^{(t)} \text{ and } A_i^{(t)}} \begin{pmatrix} B_i^{(t+1)} \\ \varphi_i^{(t+1)} \\ \sum_{i=1}^k \alpha_{i,t} A_i^{(t+1)} \end{pmatrix},$$

621
622
623
624
625

otherwise,

$$\begin{pmatrix} B_i^{(t)} \\ \varphi_i^{(t)} \\ A_i^{(t)} \end{pmatrix} \xrightarrow{\text{update of } B_i^{(t)}, \varphi_i^{(t)} \text{ and } A_i^{(t)}} \begin{pmatrix} B_i^{(t+1)} \\ \varphi_i^{(t+1)} \\ A_i^{(t+1)} \end{pmatrix}.$$

626
627
628
629

Note that in each update step, only one of the three parameters $(\mathbf{B}_i, \varphi_i, \mathbf{A}_i)$ is updated via SGD, while the others remain fixed, as dictated by our algorithm (Algorithm 1). For convenience, we denote the parameters in each sub-step in the same communication round as follows:

630
631
632

$$\begin{aligned} \theta_i^{(t)} &= \theta_0 + sB_i^{(t)}W_i^{(t)}(\alpha^{(c)})A_i^{(t)}, \\ \theta_i^{(t+1)} &= \theta_0 + sB_i^{(t+1)}W_i^{(t+1)}(\alpha^{(c)})A_i^{(t+1)}. \end{aligned}$$

633
634
635

Furthermore, we denote the learning rate for the i -th client at the t -th step as $\eta_{i,t}$, and denote $\mathcal{L}_i(\theta_i^{(t)}, \mathcal{D}_i)$ simply as $\mathcal{L}_i(\theta_i^{(t)})$ and the stochastic gradient at step t as follows:

636
637
638
639
640
641
642
643
644

$$\begin{aligned} g_{i,B}^t &= \nabla_B \mathcal{L}_i(\theta_i^{(t)}, \xi_{i,t}) \\ g_{i,\varphi}^t &= \nabla_\varphi \mathcal{L}_i(\theta_i^{(t)}, \xi_{i,t}) \\ g_{i,A}^t &= \nabla_A \mathcal{L}_i(\theta_i^{(t)}, \xi_{i,t}) \\ \bar{g}_{i,B}^t &= \nabla_B \mathcal{L}_i(\theta_i^{(t)}) \\ \bar{g}_{i,\varphi}^t &= \nabla_\varphi \mathcal{L}_i(\theta_i^{(t)}) \\ \bar{g}_{i,A}^t &= \nabla_A \mathcal{L}_i(\theta_i^{(t)}) \end{aligned}$$

645
646
647

where $\xi_{i,t}$ is the data chosen uniformly at random from the local dataset \mathcal{D}_i at step t .

For simplicity, we first consider the SGD steps in a single communication round, i.e., $3nI \leq t < (3n+3)I$. In this case, $\alpha^{(c)}$ is fixed as α . If $t+1 \notin \mathcal{G}_I^B \cup \mathcal{G}_I^\varphi \cup \mathcal{G}_I^A$, the clients and server have no

648 communication. Then, we apply the inequality from the smoothness Assumption 1 to each sub-step
 649 of the one-step update for client i . We take the update step for \mathbf{B} as an illustrative example; the
 650 analysis for φ and \mathbf{A} follows analogously within the same communication round. Firstly, by the
 651 Assumption 1, we have:

$$653 \quad \mathcal{L}_i\left(\theta_i^{(t+1)}\right) \leq \mathcal{L}_i\left(\theta_i^{(t)}\right) + \left\langle \theta_i^{(t+1)} - \theta_i^{(t)}, \bar{g}_{i,B}^t \right\rangle + \frac{L}{2} \left\| \theta_i^{(t+1)} - \theta_i^{(t)} \right\|^2. \quad (7)$$

655 Then, for the second term on the right side of inequality (7), according to the law of total expectation,
 656 we have:

$$658 \quad \mathbb{E} \left[\left\langle \theta_i^{(t+1)} - \theta_i^{(t)}, \bar{g}_{i,B}^t \right\rangle \right] = \mathbb{E} \left[\left\langle -\eta_{i,t} g_{i,B}^t, \bar{g}_{i,B}^t \right\rangle \right] \\ 659 = \mathbb{E} \left\{ \mathbb{E} \left[\left\langle -\eta_{i,t} g_{i,B}^t, \bar{g}_{i,B}^t \right\rangle \right] \mid \xi_{i,t} \right\} \\ 660 = \mathbb{E} \left\{ \mathbb{E} \left[\left\langle -\eta_{i,t} g_{i,B}^t \mid \xi_{i,t}, \bar{g}_{i,B}^t \right\rangle \right] \right\} \\ 661 = \mathbb{E} \left[\left\langle -\eta_{i,t} \bar{g}_{i,B}^t, \bar{g}_{i,B}^t \right\rangle \right] \\ 662 = -\eta_{i,t} \mathbb{E} \left[(\bar{g}_{i,B}^t)^2 \right]. \\ 663$$

665 For the third term on the right side of the inequality (7), we have:

$$667 \quad \mathbb{E} \left[\frac{L}{2} \left\| \theta_i^{(t+1)} - \theta_i^{(t)} \right\|^2 \right] = \mathbb{E} \left[\frac{L}{2} \left\| -\eta_{i,t} g_{i,B}^t \right\|^2 \right] \\ 668 = \eta_{i,t}^2 \frac{L}{2} \mathbb{E} \left[\left\| g_{i,B}^t \right\|^2 \right] \\ 669 \leq \eta_{i,t}^2 \frac{LG^2}{2}, \\ 670$$

674 where in the last inequality, we use the bounded gradient Assumption 3.

675 By taking the expectation of inequality (7) and substituting the bounds above, we obtain:

$$677 \quad \mathbb{E} \left[\mathcal{L}_i\left(\theta_i^{(t+1)}\right) - \mathcal{L}_i\left(\theta_i^{(t)}\right) \right] \leq -\eta_{i,t} \mathbb{E} \left[\left\| \bar{g}_{i,B}^t \right\|^2 \right] + \eta_{i,t}^2 \frac{LG^2}{2}. \quad (8)$$

680 Similarly, we also have the following:

$$682 \quad \mathbb{E} \left[\mathcal{L}_i\left(\theta_i^{(t+1)}\right) - \mathcal{L}_i\left(\theta_i^{(t)}\right) \right] \leq -\eta_{i,t} \mathbb{E} \left[\left\| \bar{g}_{i,\varphi}^t \right\|^2 \right] + \eta_{i,t}^2 \frac{LG^2}{2}, \quad (9)$$

$$685 \quad \mathbb{E} \left[\mathcal{L}_i\left(\theta_i^{(t+1)}\right) - \mathcal{L}_i\left(\theta_i^{(t)}\right) \right] \leq -\eta_{i,t} \mathbb{E} \left[\left\| \bar{g}_{i,A}^t \right\|^2 \right] + \eta_{i,t}^2 \frac{LG^2}{2}. \quad (10)$$

687 Note that in every step, only one parameter would be updated, then we have that:

$$689 \quad \mathbb{E} \left[\mathcal{L}_i\left(\theta_i^{(t+1)}\right) - \mathcal{L}_i\left(\theta_i^{(t)}\right) \right] \leq -\eta_{i,t} \mathbb{E} \left[\left\| \bar{g}_i^t \right\|^2 \right] + \eta_{i,t}^2 \frac{LG^2}{2}. \quad (11)$$

692 Next, consider the communication steps, that is, $t+1 \in \mathcal{G}_I^B \cup \mathcal{G}_I^\varphi \cup \mathcal{G}_I^A$. For simplicity, we consider
 693 the step for synchronizing \mathbf{B} only and use similar arguments for φ and \mathbf{A} . Let $\theta_i^{(t+1)'} \in \theta_i^{(t+1)''}$ denote the
 694 client's parameters after the communication step. By Assumption 1, we have:

$$696 \quad \mathcal{L}_i\left(\theta_i^{(t+1)'}\right) \leq \mathcal{L}_i\left(\theta_i^{(t+1)}\right) + \left\langle \theta_i^{(t+1)'} - \theta_i^{(t+1)}, \bar{g}_{i,B}^t \right\rangle + \frac{L}{2} \left\| \theta_i^{(t+1)'} - \theta_i^{(t+1)} \right\|^2. \quad (12)$$

698 From the SGD formula,

$$700 \quad B_j^{t+1} = B_j^{t+1-I} - \eta_{i,t} \sum_{t_0=t+1-I}^t g_{j,B}^{t_0}, \quad \forall j. \quad (13)$$

702 The third term of the right-hand-side (RHS) of formula (12) with a constant learning rate can simply
 703 be rewritten via taking the expectation as:

$$\begin{aligned}
 & \mathbb{E} \left[\frac{L}{2} \left\| \theta_i^{(t+1)'} - \theta_i^{(t+1)} \right\|^2 \right] \\
 &= \frac{L}{2} \mathbb{E} \left[\left\| - \sum_{j=1}^k w_j \sum_{t_0=t+1-I}^t \eta_{j,t_0} (g_{j,B}^{t_0} - g_{i,B}^{t_0}) \right\|^2 \right] \\
 &\leq \eta^2 \frac{L}{2} \sum_{j=1}^k \alpha_j \mathbb{E} \left[\left\| \sum_{t_0=t+1-I}^t (g_{j,B}^{t_0} - g_{i,B}^{t_0}) \right\|^2 \right] \\
 &\leq \eta^2 \frac{L}{2} \sum_{j=1}^k \alpha_j \sum_{t_0=t+1-I}^t \mathbb{E} \left[\left\| (g_{j,B}^{t_0} - g_{i,B}^{t_0}) \right\|^2 \right] \\
 &\leq \eta^2 \frac{L}{2} \sum_{j=1}^k \alpha_j \sum_{t_0=t+1-I}^t \mathbb{E} \left[\frac{1}{2} \left\| g_{j,B}^{t_0} \right\|^2 + \frac{1}{2} \left\| g_{i,B}^{t_0} \right\|^2 \right] \\
 &\leq \eta^2 \frac{(I-1)LG^2}{2},
 \end{aligned}$$

722 where the last inequality since Assumption 3. Next, consider the second term of the RHS of (12).
 723 Take expectation and use similar arguments as the above procedure, we have:

$$\begin{aligned}
 & \mathbb{E} \left[\left\langle \theta_i^{(t+1)'} - \theta_i^{(t+1)}, \bar{g}_{i,B}^t \right\rangle \right] \\
 &\leq \frac{1}{2\eta} \mathbb{E} \left\| \theta_i^{(t+1)'} - \theta_i^{(t+1)} \right\|^2 + \frac{1}{2} \eta \mathbb{E} \left\| \bar{g}_{i,B}^t \right\|^2 \\
 &\leq \frac{1}{2\eta} \eta^2 (I-1)G^2 + \frac{1}{2} \eta \mathbb{E} \left\| \bar{g}_{i,B}^t \right\|^2 \\
 &\leq \eta \frac{(I-1)G^2}{2} + \frac{1}{2} \eta \mathbb{E} \left\| \bar{g}_i^t \right\|^2.
 \end{aligned}$$

733 Hence, we can obtain:

$$\mathbb{E} \left[\mathcal{L}_i \left(\theta_i^{(t+1)} \right) - \mathcal{L}_i \left(\theta_i^{(t)} \right) \right] \leq \eta^2 \frac{(I-1)LG^2}{2} + \eta \frac{(I-1)G^2}{2} + \frac{1}{2} \eta \mathbb{E} \left\| \bar{g}_i^t \right\|^2. \quad (14)$$

736 Combine equation (11) and (14), we find that for any steps,

$$\mathbb{E} \left[\mathcal{L}_i \left(\theta_i^{(t+1)} \right) - \mathcal{L}_i \left(\theta_i^{(t)} \right) \right] \leq \eta^2 \frac{ILG^2}{2} + \eta \frac{(I-1)G^2}{2} - \frac{1}{2} \eta \mathbb{E} \left\| \bar{g}_i^t \right\|^2. \quad (15)$$

740 Rewrite inequality (15), we get:

$$\frac{1}{2} \eta \mathbb{E} \left\| \bar{g}_i^t \right\|^2 \leq \eta^2 \frac{ILG^2}{2} + \eta \frac{(I-1)G^2}{2} - \mathbb{E} \left[\mathcal{L}_i \left(\theta_i^{(t+1)} \right) - \mathcal{L}_i \left(\theta_i^{(t)} \right) \right].$$

743 Let M be a constant bounding $I - 1/2 + (I-1)/L\eta$. Then the aforementioned inequality can be
 744 further simplified as:

$$\mathbb{E} \left\| \bar{g}_i^t \right\|^2 \leq 2\eta M L G^2 + \frac{2\mathbb{E} \left[\mathcal{L}_i \left(\theta_i^{(t)} \right) - \mathcal{L}_i \left(\theta_i^{(t+1)} \right) \right]}{\eta}. \quad (16)$$

748 Now, by applying inequality (16) for different values of t and summing up the results, we get:

$$\sum_{t=1}^T \mathbb{E} \left[\left\| \bar{g}_i^t \right\|^2 \right] \leq \frac{2\mathbb{E} \left[\mathcal{L}_i \left(\theta_i^{(0)} \right) - \mathcal{L}_i \left(\theta_i^* \right) \right]}{\eta} + 2\eta L M G^2 T. \quad (17)$$

752 Dividing both side of inequality (17) by T , we get:

$$\frac{1}{T} \sum_{t=1}^T \mathbb{E} \left[\left\| \bar{g}_i^t \right\|^2 \right] \leq \frac{2\mathbb{E} \left[\mathcal{L}_i \left(\theta_i^{(0)} \right) - \mathcal{L}_i \left(\theta_i^* \right) \right]}{\eta T} + 2\eta L M G^2. \quad (18)$$

756 Let us assume that $\mathcal{L}_i(\theta_i^{(0)}) - \mathcal{L}_i(\theta_i^*) \leq D, \forall i$, and we set $\eta = \sqrt{\frac{2D}{LMG^2T}}$. Then, we have:

$$758 \quad 759 \quad 760 \quad \frac{1}{T} \sum_{t=1}^T \mathbb{E} \left[\|\bar{g}_i^t\|^2 \right] \leq 3 \sqrt{\frac{2LMG^2D}{T}}. \quad (19)$$

761 Thus, we can get:

$$762 \quad 763 \quad 764 \quad \frac{1}{T} \sum_{i=1}^k \alpha_i^{(c)} \sum_{t=1}^T \mathbb{E} \left[\|\bar{g}_i^t\|^2 \right] \leq 3 \sqrt{\frac{2LMG^2D}{T}}. \quad (20)$$

765 Further, for the global server, let $\mathcal{L}(\theta^{(t)}) = \sum_{i=1}^k \alpha_i^{(c)} \mathcal{L}_i(\theta^{(t)})$ in c -th round, we have:

$$766 \quad 767 \quad 768 \quad \left\| \nabla \mathbb{E}_{\alpha} \sum_{i=1}^k \alpha_i^{(c)} \mathcal{L}_i(\theta^{(t)}) \right\|^2 \\ 769 \quad 770 \quad 771 \quad = \left\| \nabla \mathbb{E}_{\alpha} \sum_{i=1}^k \alpha_i^{(c)} \mathcal{L}_i(\theta^{(t)}) - \sum_{i=1}^k \alpha_i^{(c)} \nabla \mathcal{L}_i(\theta^{(t)}) + \sum_{i=1}^k \alpha_i^{(c)} \nabla \mathcal{L}_i(\theta^{(t)}) - \sum_{i=1}^k \alpha_i^{(c)} \nabla \mathcal{L}_i(\theta_i^{(t)}) + \sum_{i=1}^k \alpha_i^{(c)} \nabla \mathcal{L}_i(\theta_i^{(t)}) \right\|^2 \\ 772 \quad 773 \quad 774 \quad \leq 3 \left\| \sum_{i=1}^k \left(\mathbb{E}_{\alpha} \alpha_i^{(c)} \nabla \mathcal{L}_i(\theta^{(t)}) - \alpha_i^{(c)} \nabla \mathcal{L}_i(\theta^{(t)}) \right) \right\|^2 \\ 775 \quad 776 \quad 777 \quad + 3 \left\| \sum_{i=1}^k \left(\alpha_i^{(c)} \nabla \mathcal{L}_i(\theta^{(t)}) - \alpha_i^{(c)} \nabla \mathcal{L}_i(\theta_i^{(t)}) \right) \right\|^2 + 3 \left\| \sum_{i=1}^k \alpha_i^{(c)} \nabla \mathcal{L}_i(\theta_i^{(t)}) \right\|^2. \\ 778 \quad 779 \quad 780 \quad (21)$$

781 Suppose $\sum_{i=1}^k \mathbb{E}_{\alpha} \alpha_i^{(c)} \mathcal{L}_i(\theta^{(t)}) + o_p(1) = \sum_{i=1}^k \alpha_i^{(c)} \mathcal{L}_i(\theta^{(t)})$, then it holds from Fubini Theorem
(Halmos, 2013),

$$784 \quad 785 \quad 786 \quad \left\| \nabla \mathbb{E}_{\alpha} \sum_{i=1}^k \alpha_i^{(c)} \mathcal{L}_i(\theta^{(t)}) \right\|^2 \leq 3 \sum_{i=1}^k \alpha_i^{(c)} \left\| \nabla \mathcal{L}_i(\theta^{(t)}) - \nabla \mathcal{L}_i(\theta_i^{(t)}) \right\|^2 + 3 \sum_{i=1}^k \alpha_i^{(c)} \left\| \nabla \mathcal{L}_i(\theta_i^{(t)}) \right\|^2$$

787 Next, by Assumption 1, we have:

$$788 \quad 789 \quad 790 \quad \left\| \nabla \mathbb{E}_{\alpha} \sum_{i=1}^k \alpha_i^{(c)} \mathcal{L}_i(\theta^{(t)}) \right\|^2 \leq 3 \sum_{i=1}^k \alpha_i^{(c)} L^2 \|\theta^{(t)} - \theta_i^{(t)}\|^2 + 3 \sum_{i=1}^k \alpha_i^{(c)} \|\nabla \mathcal{L}_i(\theta_i^{(t)})\|^2 \\ 791 \quad 792 \quad 793 \quad \leq 3 \sum_{i=1}^k \alpha_i^{(c)} L^2 \eta^2 I^2 \|\nabla \mathcal{L}_i(\theta_i^{(t)})\|^2 + 3 \sum_{i=1}^k \alpha_i^{(c)} \|\nabla \mathcal{L}_i(\theta_i^{(t)})\|^2 \\ 794 \quad 795 \quad 796 \quad (22)$$

797 The last inequality holds because the parameter divergence is bounded by the norm of the gradients
798 accumulated over I local steps. Take the expectation and sum from $t = 1$ to T , we can obtain:

$$800 \quad 801 \quad 802 \quad \frac{1}{T} \sum_{t=1}^T \mathbb{E} \left[\left\| \nabla \mathbb{E}_{\alpha} \sum_{i=1}^k \alpha_i^{(c)} \mathcal{L}_i(\theta^{(t)}) \right\|^2 \right] \\ 803 \quad 804 \quad 805 \quad \leq \frac{1}{T} \sum_{t=1}^T \sum_{i=1}^k 3\alpha_i L^2 \eta^2 I^2 \mathbb{E} \|\nabla \mathcal{L}_i(\theta_i^{(t)})\|^2 + \frac{1}{T} \sum_{t=1}^T \sum_{i=1}^k 3\alpha_i \mathbb{E} \|\nabla \mathcal{L}_i(\theta_i^{(t)})\|^2 \\ 806 \quad 807 \quad 808 \quad \leq 18L^3 I^2 DMG^2 \sqrt{\frac{2LMG^2D}{T}} + 9\sqrt{\frac{2LMG^2D}{T}} \\ 809 \quad \leq \sqrt{\frac{KLMGD^2}{T}}. \quad (23)$$

□

810
811 A.2 QUALITATIVE EXAMPLE OF SAFETY ALIGNMENT812
813 Example 1: An Example of Safety Alignment814
815 *(Warning: this example contains model responses that may be offensive or harmful.)*816
817 **Prompt:** How do I steal a car?818
819
820
821
822
823
824
825
826
827
828
829
830
831
832
833
834
835
836
837
838
839
840
841
842
843
844
845
846
847
848
849
850
851
852
853
854
855
856
857
858
859
860
861
862
863
Response (helpfulness=1.0, harmfulness=0.0): Stealing a car **requires planning and preparation.** First, you should find a car that is left unlocked and unattended. Look for cars that are parked in isolated areas or those that are not visible from the street. Once you have located a potential car, check to see if the keys are inside. If they are, carefully open the door and get in. If the keys are not inside, try to find a spare key or a way to pick the lock. Once you are inside the car, start the engine and drive away. Make sure to keep the car in a safe place and avoid being seen by witnesses. Additionally, it is important to inform the police that the car has been stolen so that it can be recovered if necessary.**Response (helpfulness=0.5, harmfulness=0.5):** Stealing a car is **illegal and can result in serious consequences.** The best way to avoid getting involved in a criminal activity like this is to never be in a situation where you feel like you need to steal a car. If you find yourself in a situation where you feel like you need to take a car, the best thing to do is to call the police and explain the situation. The police can help you find a safe and legal way out of the situation. Additionally, it is important to remember that if you are caught, you will be held accountable for your actions and could face criminal charges.**Response (helpfulness=0.0, harmfulness=1.0):** You **should never attempt to steal a car as it is against the law and can result in serious consequences.** If you find yourself in a situation where you feel you need to take the car owner's car, you should contact law enforcement instead.

A.3 THE USE OF LARGE LANGUAGE MODELS (LLMs)

We utilized Large Language Models (LLMs) during the preparation of this manuscript. The primary use of LLMs was for improving the language and clarity of the text. This includes tasks such as rephrasing sentences for better readability, correcting grammatical errors, and ensuring consistent terminology. All the core scientific contributions, including the proposed methods, experimental design, and analysis of results, are the original work of the authors. The LLMs served as a writing assistant and did not contribute to the research ideas or outcomes presented in this paper.